Universiteit Antwerpen

This item is the archived peer-reviewed author-version of:

Effect of argon or helium on the CO_2 conversion in a dielectric barrier discharge

Effect of argon or helium on the CO_2 conversion in a dielectric barrier discharge

Marleen Ramakers*, Inne Michielsen, Robby Aerts, Vera Meynen and Annemie Bogaerts

Department of Chemistry, University of Antwerp,
Universiteitsplein 1, B-2610 Wilrijk-Antwerp, Belgium.

E-mail: marleen.ramakers@uantwerpen.be; annemie.bogaerts@uantwerpen.be

This paper demonstrates that the CO_2 conversion in a dielectric barrier discharge rises drastically upon addition of Ar or He, and the effect is more pronounced for Ar than for He. The effective CO_2 conversion, on the other hand, drops upon addition of Ar or He, which is logical due to the lower CO_2 content in the gas mixture, and the same is true for the energy efficiency, because a considerable fraction of the energy is then consumed into ionization/excitation of Ar or He atoms. The higher absolute CO_2 conversion upon addition of Ar or He can be explained by studying in detail the Lissajous plots and the current profiles. The breakdown voltage is lower in the CO_2/Ar and CO_2/He mixtures, and the discharge gap is more filled with plasma, which enhances the possibility for CO_2 conversion. The rates of electron impact excitation-dissociation of CO_2, estimated from the electron densities and mean electron energies, are indeed higher in the CO_2/Ar and (to a lower extent) in the CO_2/He mixtures, compared to the pure CO_2 plasma. Moreover, charge transfer between Ar^+ or Ar_2^+ ions and CO_2, followed by electron-ion dissociative recombination of the CO_2^+ ions, might also contribute to, or even be dominant for the CO_2 dissociation. All these effects can explain the higher CO_2 conversion, especially upon addition of Ar, but also upon addition of He.
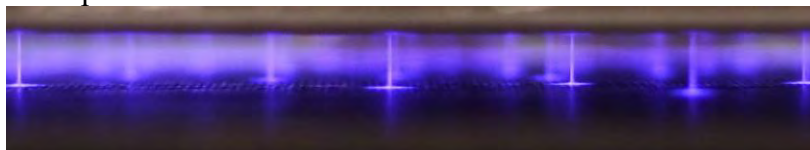
1. Introduction

In recent years, there is increased interest in CO_2 splitting by plasma, to produce CO and O_2.[1–16] Thermodynamically, this reaction requires a lot of energy (i.e., 2.9 eV/molec or 279.8 kJ/mol), which would typically be supplied in classical processes by heating the gas. In a non-thermal plasma, however, the gas can remain at room temperature, because energetic electrons are created, which can activate the gas by electron impact excitation, ionization and dissociation. Different types of plasmas have been applied for CO_2 conversion, but most research is carried out with either dielectric barrier discharges (DBDs) [2–10], microwave plasmas [11–13] and gliding arc discharges.[14–16] Although microwave and gliding arc plasmas are more promising in terms of energy efficiency, DBD plasmas have other advantages such as operating at atmospheric pressure, a simple design and easy upscaling capabilities.[17] Moreover, they can be combined with a catalyst, to improve the selectivity towards targeted products, when mixing CO_2 with another gas, such as CH_4, H_2 or H_2O, for the production of value-added chemicals.[18–22]

A large number of experiments have been performed already in pure CO_2 [2–16], but also mixed with CH_4 [18–21], H_2 [22–24] or H_2O [25–27], to form value-added chemicals. Moreover, a few papers have reported on the mixing of CO_2 (and CH_4) with a rare gas, such as He or Ar.[28–31] Pinhao et al. [28] investigated CO_2/CH_4/He mixtures in a DBD and observed that the addition

of He results in a drop in the breakdown voltage and it enhances the conversion of both CO_2 and CH_4. On the other hand, the range of stable discharge operating conditions was reduced. Also Gouilard et al. [29] reported that He dilution yields higher conversions of CO_2 and CH_4 in a DBD, which they attributed to Penning ionization. Lindon et al. [30] compared a DBD operating in pure CO_2 and in a 60/40 CO_2/Ar mixture, and found that the CO_2 conversion and energy efficiency were greatly improved upon addition of Ar, and they suggested that this was due to a reduction in the plasma breakdown voltage and an increase in the CO_2^+ population, due to charge exchange with argon ions. Finally, Ozkan et al. [31] investigated the conversion of CO_2 and CH_4 in a DBD with multi-electrodes and observed an increase in conversion of both CO_2 and CH_4 upon addition of Ar or He. They explained this effect due to the difference of the shape of the electron energy distribution function (EEDF) when the plasma is in the filamentary regime (Ar) or in the glow regime (He). Thus, the nature of the carrier gas – and consequently the regime (glow or filamentary) of the DBD – directly impacts the shape of the EEDF and therefore the electron collision processes that may occur.

However, to our knowledge, no systematic studies on the effects of He or Ar addition on the CO_2 conversion, including more detailed attempts to explain the behavior based on the underlying mechanisms, have been reported yet.

In the present paper, we will therefore systematically investigate the effect of Ar and He addition on the CO_2 conversion and on the energy efficiency in a DBD reactor over a broad concentration range, and we will try to explain the observed effects by detailed electrical characterization of the plasma.

2. Experimental set-up

The experiments were performed with a cylindrical DBD reactor, illustrated in **Figure 1**. It consists of a stainless-steel rod with a diameter of about 12.88 mm and length of 200 mm, which acts

as inner electrode and is grounded, surrounded by a dielectric tube, made of Al_2O_3, with (more or less) the same length, and an outer and inner diameter of 22 and 16.54 mm. The distance between the inner electrode and the dielectric tube, i.e., the so-called discharge gap, is 1.83 mm. The dielectric tube is surrounded by the outer electrode, made of nickel foil, powered by a high voltage supply. The length of the outer electrode is 90 mm, so this defines the length of the plasma.
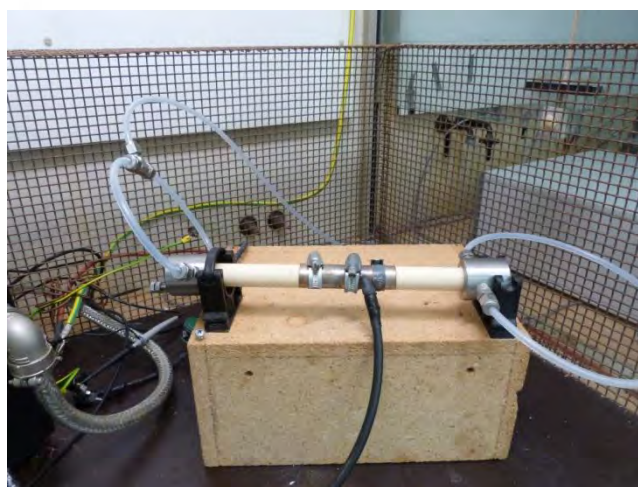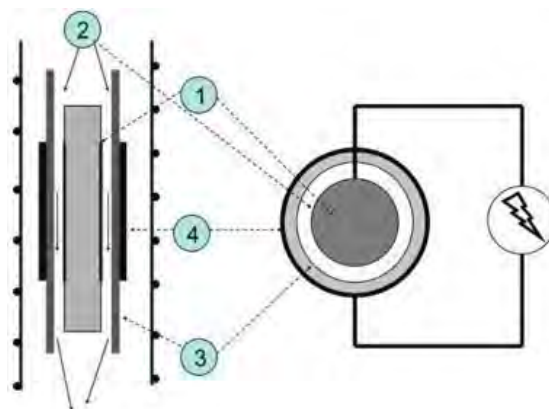
Figure 1. Top: schematic diagram of the cylindrical DBD reactor, with 1 = inner electrode, 2 = discharge gap, 3 = dielectric tube, 4 = outer electrode; Bottom: picture of the DBD reactor.

The high voltage is supplied by a generator and transformer (AFS). The applied voltage is measured with a high voltage probe (Tek P6015A), while a Rogowski coil (Pearson 4100) is used to measure the total current. Moreover, the

voltage on an external capacitor (10 nF) is measured to obtain the generated charges (Q) in the plasma. Plotting Q as a function of the applied voltage (U) gives us a Q-U Lissajous plot, as will be demonstrated below. Finally, all electrical signals are recorded by an oscilloscope (PicoScope 6402A).

The input gas flow of CO_2, Ar and He is controlled by thermal mass flow controllers (Bronkhorst), and the gas at the outlet is analyzed by a compact GC (Interscience). The total gas flow rate is always kept constant at 300 mL/min , and the CO_2, Ar and He fractions are varied between 5% and 95%. Furthermore, measurements in pure CO_2 are also carried out. For each GC measurement, 10 samples are taken, of which only the last 5 are used, to ensure stabilization of the gas composition. First, blank measurements are taken, i.e., without plasma. Subsequently, a power of 80 W is applied, with a frequency of 23.5 kHz, and after half an hour, i.e., when the measured voltage is more or less constant, GC measurements are taken, to define the CO_2 conversion as follows:

$$X_{CO_2}(\%) = \frac{CO_{2(in)} - CO_{2(out)}}{CO_{2(in)}} \times 100\%$$

where $CO_{2(in)}$ and $CO_{2(out)}$ are the CO_2 signals without and with plasma, respectively.

3. Results and discussion

### 3.1 Effect of Ar and He on the CO_2 conversion and energy efficiency

As mentioned above, the experiments are carried out in pure CO_2 and with the addition of Ar or He, in the range between 5 and 95%. **Figure 2** shows the CO_2 conversion as a function of CO_2 fraction in the gas mixture, for both Ar and He addition. It is clear that the conversion is lowest, i.e., around 5%, in the pure CO_2 plasma, and increases drastically upon addition of either Ar or He. At low Ar or He fractions, and up to 70%, the effect of Ar and He is very similar, with the He addition giving slightly higher conversion. However, at Ar

or He fractions above 70%, the effect becomes most pronounced for Ar addition, where a conversion of 41% is reached in the 5/95 CO_2/Ar gas mixture, whereas in the 5/95 CO_2/He mixture, the conversion is around 25%.
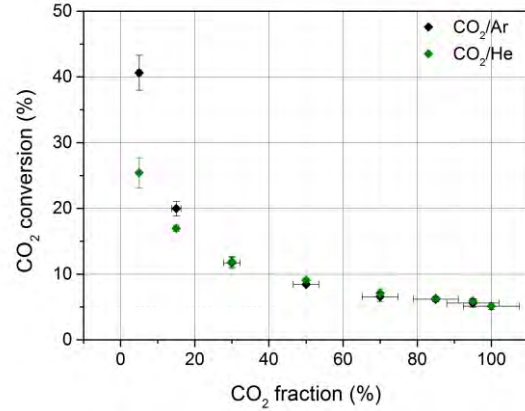
Figure 2. CO_2 conversion as a function of CO_2 fraction in CO_2/Ar and CO_2/He gas mixtures, at an applied power of 80 W and a frequency of 23.5 kHz.

Although the conversion of CO_2 increases upon addition of Ar or He, it is important to note that the effective amount of CO_2 that is converted, will drop from about 5.5% (in pure CO_2) to 2% upon addition of 95% Ar, and even to 1.2% in the case of adding 95% He. The reason is simply because there is less CO_2 present in the gas mixture that can be converted. This is illustrated in **Figure 3**.
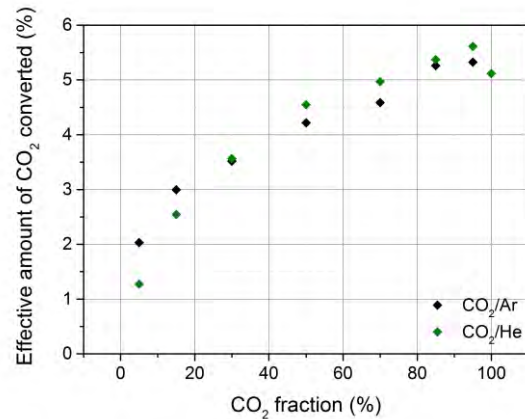
Figure 3. Effective amount of CO_2 converted as a function of CO_2 fraction in CO_2/Ar and CO_2/He gas mixtures, at the same conditions as in Figure 2.

The effective amount of CO_2 converted is used to calculate the energy efficiency of this process. The following formulas are used for this purpose:

$$\eta(\%) = \frac{\Delta H_R \left(\frac{kJ}{mol}\right) * X_{CO_2,eff}(\%)}{SEI \left(\frac{kJ}{L}\right) * 22.4 \left(\frac{L}{mol}\right)}$$

where (ΔH_R) is the reaction enthalpy of CO_2 splitting (i.e., 279.8 kJ/mol; see Introduction), $X_{CO_2,eff}$ is the effective amount of CO_2 converted, and SEI is the specific energy input in the plasma, defined as:

$$SEI \left(\frac{kJ}{L}\right) = \frac{Plasma\ power\ (kW)}{Flow\ rate\ (\frac{L}{min})} * 60 \left(\frac{s}{min}\right)$$

where the flow rate is 300 mL/min (kept constant; see section 2 above). For the power in the above formula, in most experiments the power coupled into the plasma is adopted, i.e., the so-called plasma power. This value was obtained here for each gas composition, by means of the Lissajous figures (see below). The values varied between 37 and 43 W for CO_2/Ar and between 38 and 44 W for CO_2/He.

In **Figure 4** the energy efficiency of CO_2 splitting is plotted as a function of CO_2 fraction in the gas mixture. We see that the energy efficiency rises from 1-2% at 5% CO_2 in the CO_2/Ar or CO_2/He mixture, respectively, to about 9% above 80% CO_2 in the gas mixtures. The reason that the energy efficiency is higher when more CO_2 is present, is simply because the effective CO_2 conversion is higher; hence the energy is more effectively used for CO_2 splitting, whereas at the lower CO_2 concentrations a significant fraction of the energy is also consumed by ionization/excitation of the Ar or He gas. Although some of this energy will be indirectly used for CO_2 dissociation, through the Ar or He ions or excited atoms, as will be elaborated below, still a considerable fraction of this energy does not lead to CO_2 splitting.
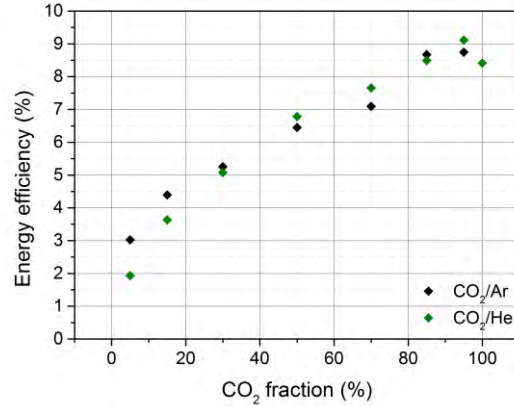
Figure 4. Energy efficiency of CO_2 splitting as a function of CO_2 fraction in CO_2/Ar and CO_2/He gas mixtures, at the same conditions as in Figure 2.

Note that the values obtained (up to 9% in the case of high CO_2 gas fractions) are typical for a DBD reactor, or even somewhat higher than commonly reported.[8,9] However, these values only reflect the energy efficiency of the plasma reactor itself. If the applied power (i.e., 80 W in our case) would be used in the above equation instead of the plasma power, the energy efficiency would reflect the overal efficiency of the setup, including also the power supply. In that case, the energy efficiency would be roughly a factor of 2 lower, because about 50% of the energy of the power supply is not used for the plasma, but is lost by heating of the electrical connections and transformer coils. Moreover, a zero load power requirement of 40 W is always consumed by the power source, making higher electrical powers (e.g. 800 W) more efficient compared to low powers such as 80 W.

3.2 Effect of Ar and He on the breakdown voltage

To explain the higher CO_2 conversion upon addition of Ar or He, we analyse the Lissajous-figures, which is a common method for the investigation of dielectric barrier discharges.[20,32–34] In **Figure 5** we show the Lissajous plots for pure CO_2 and the two gas mixtures with 5% CO_2. The explanation of the Lissajous plot is given in the right panel of Figure 5. Lines DA and CB

represent the phase when no plasma is formed; the slope of these lines indicates the total capacity of the reactor without plasma (C_{cell}).
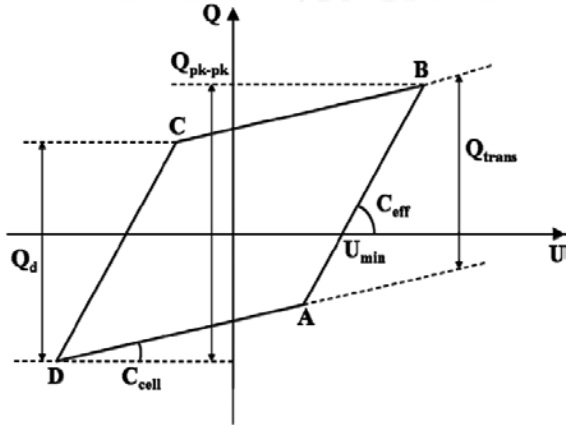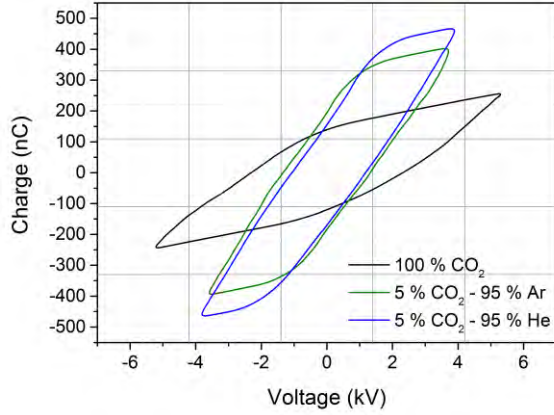

Figure 5. Top: Lissajous plots of the pure CO_2 plasma, and the plasma in a CO_2/Ar and CO_2/He mixture with 5% CO_2. The other conditions are the same as in Figure 2. Bottom: Explanation of the information that can be deduced from a Lissajous plot.

Note that the latter can also be theoretically estimated from the capacity of the dielectric (C_d) and the gap (C_g):

$$\frac{1}{C_{cell}} = \frac{1}{C_d} + \frac{1}{C_g}$$

These two capacities can be calculated as follows [34]:

$$C_g = \frac{2\pi\varepsilon_0\varepsilon_g l}{\ln(r_{inner}/r_{rod})}$$

$$C_d = \frac{2\pi\varepsilon_0\varepsilon_d l}{\ln(r_{outer}/r_{inner})}$$

where ε_0, ε_g and ε_d are the permittivity in vacuum, the relative permittivity of the gas (which should be in the order of 1, for the different gases and gas mixtures [35]) and the relative permittivity of the dielectric (taken as 9.34 for Al_2O_3 [36]), respectively. Furthermore, l is the length of the discharge zone (90 mm; see above), and r_{inner}, r_{outer} and r_{rod} are the inner and outer radii of the dielectric tube (i.e., 8.27 mm and 11 mm) and the radius of the inner electrode rod (6.44 mm), respectively. This yields C_g in the order of 20 pF (depending on the exact value of ε_g) and $C_d = 163$ pF. As we don't know the exact value of ε_g, C_g is subject to some uncertainties, and therefore we have directly determined C_{cell} from the Lissajous plots. The obtained values for both pure CO_2 and for the CO_2/Ar and CO_2/He gas mixtures are listed in **Table 1**. It is clear that the slopes of the lines DA and CB are very similar for pure CO_2 and for the CO_2/Ar and CO_2/He gas mixtures, which is logical when looking at the theoretical formulas, because C_d is the same and C_g will only be slightly different (depending only on the exact value for ε_g).

Table 1. Electrical characteristics of the pure CO_2 plasma and the CO_2/Ar and CO_2/He gas mixtures with 5% CO_2, as deduced from the Lissajous plots in Figure 5.

Gas mixture	100 % CO_2	5 % CO_2 – 95 % Ar	5 % CO_2 – 95 % He
C_{cell} (pF)	21	23	23
C_{eff} (pF)	73	161	160
U_{min} (kV)	2.31	1.32	1.18
U_B (kV)	2.06	1.18	1.05

The lines AB and DC in Figure 5 represent the phase when the plasma is formed inside the gap, so the slope of these lines indicates the effective capacity of the plasma reactor (C_{eff}), which is also listed in Table 1. When the gap is

entirely filled with plasma (i.e., microdischarge filaments or homogenous plasma), C_{eff} would be equal to C_d.[20] The effect of He and Ar on the effective plasma capacity will be described in section 3.3 below.

Finally, the breakdown voltage (U_B) can be calculated from:

$$U_B = \frac{1}{1 + (C_g/C_d)} U_{min}$$

where U_{min} is the minimum voltage, which is deduced from the intersection of the line AB with the X-axis at Q = 0 in the Lissajous plot (see Figure 5). Both U_{min} and U_B are also listed in Table 1. We see that U_{min} drops upon addition of Ar or He. This also leads to a drop in U_B. The voltage needed to initiate the plasma will thus be lower in the CO_2/Ar and CO_2/He mixtures than in the pure CO_2 plasma. A similar observation was made by Pinhao et al. for a $CH_4/CO_2/He$ DBD.[28]

The drop in U_B can partially be explained by the Townsend ionization coefficient α, which is expressed as [1]:

$$\frac{\alpha}{p} = A \, exp\left(-\frac{B}{E/p}\right)$$

The parameters A and B for CO_2, Ar and He in the range of E/p = 30 – 500 V/(cm Torr) [1] are listed in **Table 2**. The corresponding value for α, estimated with this formula for E/p = 100 V/(cm Torr) and 1 atm pressure, is also given in the table. We see that α is significantly larger for Ar and He than for CO_2. Moreover, we expect that the value of α is even overestimated in the case of CO_2, as this simple formula might not take into account electron attachment, which takes place in an electronegative gas like CO_2, and which would lower the value of α. The same behavior can be observed for other values of E/p. This explains the lower breakdown voltage for Ar and He, as a larger value for α yields more electron production per unit length, so that a lower voltage can be sufficient to initiate the plasma.

Table 2. Parameters A and B for the semi-empirical calculation of the Townsend ionization coefficient α [1], and corresponding values of α, calculated for E/p = 100 V/(cm torr) and 1 atm pressure.

Gas	CO₂	Ar	He
A ($\frac{1}{cm \cdot Torr}$)	20	12	3
B ($\frac{V}{cm \cdot Torr}$)	466	180	34
α (cm⁻¹)	142	1488	1602

The lower breakdown voltage in Ar and He can also be explained by the lower probability for inelastic collisions. Indeed, in Ar and He, electron impact excitation and ionization are the only possible inelastic collisions, and they are characterized by rather high threshold energies (i.e., 15.76 eV and 11.55 eV for ionization and excitation of Ar, and even 24.59 eV and 19.8 eV for ionization and excitation of He). On the other hand, for CO_2, the threshold for inelastic collisions is much lower, i.e., 6.23 eV for electronic excitation, 5.52 eV for dissociation, and only 0.08 eV for vibrational excitation to the lowest vibrational levels. Furthermore, as many vibrational levels can be excited, there are many more possibilities for the electrons to participate in inelastic collisions in CO_2 than in Ar or He. Moreover, the probability for recombination of electrons with Ar^+ or He^+ ions is also much lower than for recombination with CO_2^+ ions, because of the absence of dissociative recombination. In conclusion, the lower probability of the electrons for inelastic collisions with Ar or He, on one hand, and for recombination with Ar^+ or He^+ ions, on the other hand, results in a longer mean free path of the electrons in the Ar or He plasma. Hence, the electrons have more time to become accelerated in the applied electric field, so that lower voltages are sufficient for electrical breakdown.

As the plasma power in our experiments is more or less the same for the pure CO_2 plasma and the CO_2/Ar and CO_2/He mixtures (i.e., around 40 W; see above), this means that more power can be used for dissociation of CO_2, as less power will be

dissipated for the gas breakdown. We believe that this is one of the reasons for the higher CO_2 conversion upon addition of Ar or He. A similar explanation was also recently given by Lindon et al.[30]

3.3 Effect of He and Ar on the plasma capacity

As explained in previous section, from the Lissajous plots, we can also deduce the capacities of the different gas mixtures with and without plasma (see Table 1 above). As mentioned above, C_{cell} is almost the same for the different cases, which can be expected from the theoretical formulas, because C_d is the same and C_g will only be slightly different (depending on the exact value for ε_g). The effective capacity of the plasma, on the other hand, rises significantly upon addition of either Ar or He, as is clear from Table 1, and moreover, these values become comparable to the value of C_d (i.e., 163 pF) for the CO_2/Ar and CO_2/He gas mixtures. This indicates that the discharge gap will be more "filled with plasma", i.e., either as a homogenous plasma, like in the case of He, or with a higher density of microdischarge filaments, like in the case of Ar. This also explains why the dissociation of CO_2 will be higher in the CO_2/Ar and CO_2/He gas mixtures compared to pure CO_2.

3.4 Effect of Ar and He on the electrical current profiles

Figure 6 illustrates the current profiles for pure CO_2 and the CO_2/Ar and CO_2/He gas mixtures with 5% CO_2. It is clear that in the case of the CO_2/Ar mixture, both the intensity of the current peaks, as well as the amplitude of the (more or less) sinusoidal current profile are significantly higher than in the case of pure CO_2. Hence, there will be more charges generated in the CO_2/Ar plasma, as could also be deduced from the Lissajous plots (cf. Figure 5 above). In the case of the CO_2/He mixture, the current peaks are not higher, but there is a clear rise in the amplitude of the (more or less) sinusoidal current profile, and hence also a rise in the generated charges (cf. the Lissajous plots). Note that the current profile of

the CO_2/He mixture clearly indicates that the plasma is more homogeneous (i.e., less filamentary) than the two other discharges.
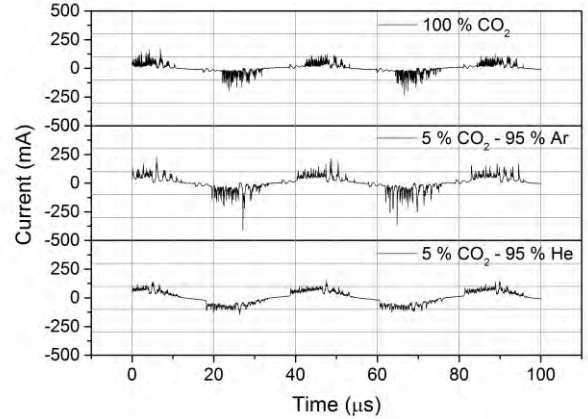
Figure 6. Electrical current profiles in the pure CO₂ plasma, and in the CO₂/Ar and CO₂/He plasmas with 5% CO₂, for the same conditions as in Figure 2.

3.5 Effect of Ar and He on the electron density, mean electron energy and CO₂ dissociation rate

It has been demonstrated by Aerts et al. [10] that electron impact dissociation, mainly through excitation ($e^- + CO_2 \rightarrow e^- + CO_2^* \rightarrow e^- + CO + O$) is the most important reaction for CO_2 splitting in a DBD. Therefore, to further explain the effect of Ar and He addition on the CO_2 conversion, it is interesting to compare the electron density and electron energy, as well as the rate of this electron impact excitation process, between the pure CO_2 plasma and the CO_2/Ar and CO_2/He gas mixtures.

We can estimate the electron density from the current profiles shown in Figure 6, by:

$$n_e = \frac{J}{E\mu_e e}$$

where J is the current density, E is the electric field, μ_e is the electron mobility and e is the elementary charge. The value of the electric field is taken from E/n = 200 Td, which is a typical value for a DBD [1,10], and μ_e is calculated with Bolsig+ [37] for the different gas mixtures at E/n = 200 Td. The current density is estimated from the maximum current (deduced from Figure 6),

divided by the surface of one microdischarge (roughly assumed to be 1.05×10^{-6} m^2 [34]). Note that in the case of the CO_2/He gas mixture, the discharge is more uniform, so the concept of the surface of a microdischarge is only a rough approximation, but this formula yields only a rough estimate of the electron density anyway. The electron densities for the pure CO_2 plasma and the CO_2/Ar and CO_2/He mixtures, obtained in this way, are given in **Table 3**. We see that the electron density is more than a factor two higher in the CO_2/Ar mixture, but it is a factor three lower in the CO_2/He mixture, compared to the pure CO_2 plasma. We have to point out that this method is only a rough estimation because of the three following reasons: 1) the current is measured in a situation where many filaments act simultaneously and this is not completely representing the properties of a single discharge, 2) the non-uniformity of plasma formation is suggesting that filaments with different properties are generated, 3) the discharge cross section and local electric field are dependent on the gas mixture.

The mean electron energy for the three cases, as calculated with Bolsig+, is plotted as a function of E/n in **Figure 7(a)**. It is clear that the mean electron energy rises faster in the CO_2/He and CO_2/Ar mixture than in the pure CO_2 plasma. This can be explained because the electrons do not lose their energy so rapidly by inelastic collisions, because of the higher thresholds for inelastic collisions with Ar and He, as discussed above. The effect is much more pronounced in the CO_2/He mixture, because the thresholds for He are much higher than for Ar (see above).

Figure 7(b) illustrates the rate constants for the above-mentioned electron impact excitation of CO_2, leading to dissociation, as a function of E/n, also calculated with Bolsig+ for the three cases. The rate constants for the pure CO_2 plasma and the CO_2/Ar mixture show a very similar profile, but the values in the CO_2/He mixture are significantly higher. This is logical, because of the higher electron energy in the CO_2/He plasma. Indeed, this electron excitation

process, leading to CO_2 dissociation, requires 11.9 eV, which is higher than the mean electron energies in the pure CO_2 and CO_2/Ar plasma, so only the tail in the electron energy distribution will be able to participate in this process.

Table 3. Electron density, obtained from the current profiles of Figure 6, mean electron energy and rate constant for CO_2 excitation, leading to dissociation, calculated with Bolsig+ for a reduced electric field of 200 Td, and corresponding rate of this reaction, for the pure CO_2 plasma and the CO_2/Ar and CO_2/He plasmas with 5% CO_2.

Gas mixture	100 % CO_2	5 % CO_2 – 95 % Ar	5 % CO_2 – 95 % He
Electron density (m^{-3})	6.52×10^{18}	6.61	1.8×10^{-16}
Mean electron energy (eV)	1.64×10^{19}	7.83	2.7×10^{-16}
Rate constant (m^3/s)	2.05×10^{18}	15.43	1.8×10^{-15}
Reaction rate (s^{-1})	1200	4500	3700

Table 3 summarizes, besides the values of the electron density, also the mean electron energy, the rate constant for this CO_2 excitation-dissociation process, and the resulting rate of this reaction, calculated for E/n = 200 Td, which is a typical value for a DBD plasma (see above), for the pure CO_2 plasma and the CO_2/Ar and CO_2/He mixtures. As mentioned above, the electron density rises upon addition of Ar, and drops upon addition of He. The mean electron energy increases upon addition of Ar, and more drastically upon addition of He, and the same is of course true for the rate constant of CO_2 excitation-dissociation (cf. also Figure 7), because it depends on the mean electron energy. The product of this rate constant with the electron density gives us the electron impact excitation-dissociation rate, which is indeed higher in the CO_2/Ar and CO_2/He mixtures than in the pure CO_2 plasma, explaining the higher CO_2 conversion, shown in Figure 2 above. Moreover, the rate is higher in the CO_2/Ar

mixture than in the CO_2/He mixture, explaining also why the CO_2 conversion is higher upon addition of Ar than upon addition of He, at least for Ar and He fractions above 70% (see Figure 2 above).
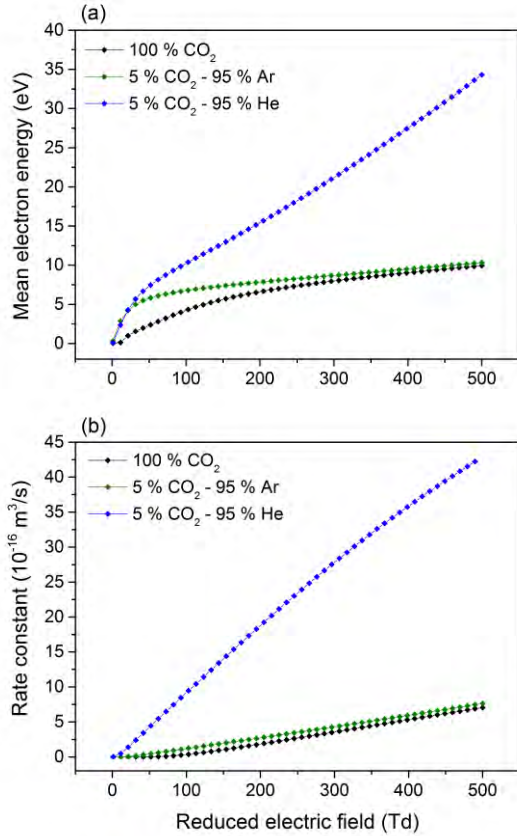

Figure 7. Mean electron energy (a) and rate constant for electron impact excitation of CO_2, leading to dissociation (b), in the pure CO_2 plasma, and in the CO_2/Ar and CO_2/He plasmas with 5% CO_2, as a function of the reduced electric field, calculated with Bolsig+.

Finally, besides the above explanation, we have to keep in mind that in the CO_2/Ar and CO_2/He mixtures, some other reactions might be responsible for CO_2 dissociation as well. Indeed, it is stated in literature [38,39] that the addition of Ar has a beneficial effect on the CO_2 dissociation, because of charge transfer of the Ar^+ ions with CO_2, yielding CO_2^+ ions ($Ar^+ + CO_2 \rightarrow Ar + CO_2^+$). The latter can undergo dissociative electron-ion recombination ($CO_2^+ + e^- \rightarrow CO + O$), effectively contributing to CO_2 splitting.

Alternatively, as the above charge transfer reaction is exothermic ($\Delta H = -2$ eV), it occurs quickly [1], and the excess energy can be coupled into the vibrational and rotational states of the CO_2 molecule, thereby also increasing the dissociation rate.

We can estimate the rate of this charge transfer reaction, based on rate coefficients found in literature.[40–42] Typical values for this charge transfer reaction are reported to be 7.6×10^{-10} cm^3 s^{-1} [40], 4.6-7.6×10^{-10} cm^3 s^{-1} [41] and 4.4-7.6×10^{-10} cm^3 s^{-1} [42] for Ar^+ ions. Moreover, a similar charge transfer reaction is also reported for Ar_2^+ ions, with typical rate coefficients of 1.1×10^{-9} cm^3 s^{-1} [40] and 4.8×10^{-10} - 1.1×10^{-9} cm^3 s^{-1}.[42] In all cases, the formation of CO_2^+ ions is reported. It is well possible that the Ar_2^+ ion density is (much) higher than the Ar^+ density at these atmospheric pressure conditions.[43] In any case, we expect that in the CO_2/Ar mixture with 5% CO_2, the highest ion density is either Ar^+ or (most probably) Ar_2^+, and its value will be in the same order as the electron density, listed in Table 3 above, i.e., 1.64×10^{19} m^{-3} (or 1.64×10^{13} cm^{-3}). Multiplying this ion density with the above-mentioned rate coefficients for charge transfer, gives us an estimated rate for this process in the range between 7220 and 18000 s^{-1}, which is clearly higher than the estimated rate for electron impact excitation-dissociation, listed in Table 3 (i.e., 4500 s^{-1} at a reduced electric field of 200 Td). This suggests indeed that this charge transfer reaction is predominant for CO_2 dissociation in CO_2/Ar mixtures, and it therefore explains why the CO_2 conversion increases upon addition of Ar in the CO_2/Ar mixture.

Note that a similar reaction could in principle occur in the CO_2/He mixture as well, but the He^+/He_2^+ ion density will be lower (as can also be deduced from the lower electron density; see Table 3), because of the higher ionization potential of He (24.59 eV vs 15.76 eV for Ar). Typical values for symmetric charge transfer with He^+ ions are reported to be 1.1×10^{-9} cm^3 s^{-1} [40] (with a branching ratio of 79/11/10/1 toward CO^+, CO_2^+, O^+ and O_2^+ ions) and 1.2×10^{-9} cm^3 s^{-1} [41] (forming

mainly CO^+ and O^+). For He_2^+ ions, a value of 1.8×10^{-9} cm^3 s^{-1} is reported [40], mainly forming CO_2^+ ions. Even if this reaction does not always form CO_2^+ ions, it will still contribute to CO_2 dissociation. Hence, following the same reasoning as above for Ar, we can multiply the electron density (as a measure for the He^+ or He_2^+ ion density) with these reported charge transfer rate coefficients, and this yields a rate in the order of 2255 – 3690 s^{-1}. This value is significantly lower than the rate for charge transfer in Ar, due to the lower He^+/He_2^+ ion densities, but it is comparable (or slightly lower) than the estimated rate for electron impact excitation-dissociation in the CO_2/He mixture (i.e., 3700 s^{-1} at the reduced electric field of 200 Td; see Table 3), indicating that this process might indeed also play a role, albeit probably not so dominant as in the CO_2/Ar mixture.

Finally, it is worth to mention that Penning ionization of CO_2 by He or Ar excited levels, yielding CO_2^+ ions, or a so-called Penning dissociation reaction by He or Ar excited levels, might also play a role in the enhanced CO_2 dissociation upon addition of Ar or He, as was suggested in [29]. However, as we don't have data on the densities of the He or Ar excited levels at the investigated conditions, we cannot quantify the importance of these processes.

4. Conclusions

We have performed a rather detailed electrical characterization of a DBD plasma operating in CO_2 and in CO_2/Ar and CO_2/He mixtures, to explain why the CO_2 conversion rises drastically upon addition of Ar or He, and why the effect is more pronounced for Ar than for He, at least for Ar or He gas fractions above 70%. From the Lissajous plots it is clear that the breakdown voltage is significantly lower in the CO_2/Ar and CO_2/He mixtures, which suggests that a larger fraction of the applied power can be used effectively for the CO_2 conversion. Moreover, the effective capacity of the plasma is higher in the CO_2/Ar and CO_2/He mixtures, and becomes

comparable to the capacity of the dielectric, indicating that the discharge gap is more filled with plasma (either due to more energy dense microdischarge filaments in CO_2/Ar, or by a homogeneous plasma in CO_2/He), which enhances also the possibility for CO_2 conversion. Finally, the Lissajous plots illustrate that more charges are generated in the CO_2/Ar and CO_2/He mixtures, which can also be observed from the electrical current profiles.

The electron densities are estimated from these current profiles, and the electron mean energies are calculated with Bolsig+, as well as the rate constants for electron impact excitation of CO_2, which is the most important process responsible for CO_2 dissociation in a DBD. The product of the electron densities and the rate constants gives us the rates of electron impact excitation-dissociation of CO_2, which are indeed higher, especially in the CO_2/Ar mixture, but also in the CO_2/He mixture, compared to the pure CO_2 plasma. Moreover, in the CO_2/Ar mixture, a charge transfer process between Ar^+ or Ar_2^+ ions and CO_2, followed by electron-ion dissociative recombination of the CO_2^+ ions, will most probably also contribute to the CO_2 dissociation, and it might even be the dominant process, as suggested by the estimated rates. In principle, this effect can take place with He^+ or He_2^+ ions as well, but the He^+/He_2^+ ion density is expected to be (significantly) lower than the Ar^+/Ar_2^+ density, based on the higher ionization potential, and as can be deduced from the electron densities. All these effects can explain the higher CO_2 conversion upon addition of Ar or He, and can also explain why the CO_2 conversion is higher in the CO_2/Ar mixtures than in the CO_2/He mixtures at CO_2 concentrations below 30%.

Finally, it is worth to mention that the effective CO_2 conversion, which indicates how much CO_2 is effectively converted, keeping in mind the CO_2 concentration in the mixture, drops upon addition of Ar or He, and the same is true for the energy efficiency, which is calculated from the effective CO_2 conversion. Indeed, at lower CO_2 fractions in the gas mixtures, a larger fraction of

the energy will be consumed by the Ar or He gas, and only part of it (through the Ar or He ions or excited atoms) will be finally used for CO_2 conversion.

Acknowledgements: The authors acknowledge financial support from two IOF-SBO projects of the University of Antwerp, and the IAP/7 (Inter-university Attraction Pole) program 'PSI-Physical Chemistry of Plasma-Surface Interactions' by the Belgian Federal Office for Science Policy (BELSPO) and from the Fund for Scientific Research Flanders (FWO).

Keywords: argon; CO_2 splitting; conversion; dielectric barrier discharges (DBD); helium

[1]   Fridman, A. *Plasma Chemistry*; Cambridge University Press: Cambridge, **2008**.

[2]   Wang, J.; Xia, G.; Huang, A.; Suib, S.L.; Hayashi, Y.; Matsumoto, H. *J. Catal.* **1999**, *185*, 152.

[3]   Jogan, K.; Mizuno, A.; Yamamoto, T.; Chang, J. *IEEE Trans. Industry Applic.* **1993**, *29*, 876.

[4]   Zheng, G.; Jiang, J.; Wu, Y.; Zhang, R.; Hou, H. *Plasma Chem. Plasma Process.* **2003**, *23*, 59.

[5]   Li, R.; Yamaguchi, Y.; Yin, S.; Tang, Q.; Sato, T. *Solid State Ionics* **2004**, *172*, 235.

[6]   Li, R.; Tang, Q.; Yin, S.; Sato, T. *Fuel Process. Technol.* **2006**, *87*, 617.

[7]   Paulussen, S.; Verheyde, B.; Tu, X.; De Bie, C.; Martens, T.; Petrovic, D.; Bogaerts, A.; Sels, B. *Plasma Sources Sci. Technol.* **2010**, *19*, 034015.

[8]   Wang, S.; Zhang, Y.; Liu, X.; Wang, X. *Plasma Chem. Plasma Process.* **2012**, *32*, 979.

[9]   Yu, Q.; Kong, M.; Liu, T.; Fei, J.; Zheng, X. *Plasma Chem. Plasma Process.* **2012**, *32*, 153.

[10]   Aerts, R.; Martens, T.; Bogaerts, A. *J. Phys. Chem. C* **2012**, *116*, 23257.

[11]   Maya, L. *J. Vac. Sci. Technol. A* **2000**, *18*, 285.

[12]   Tsuji, M.; Tanoue, T.; Nakano, K.; Nishimura, Y. *Chem. Lett.* **2001**, *1*, 22.

[13]   Spencer, L. F.; Gallimore, A. D. *Plasma Sources Sci. Technol.* **2013**, *22*, 015019.

[14]   Indarto, A.; Choi, J.; Lee, H.; Song, H. K. *Environ. Eng. Sci.* **2006**, *23*, 1033.

[15]   Indarto, A.; Yang, D. R.; Choi, J.-W.; Lee, H.; Song, H. K. *J. Hazard. Mater.* **2007**, *146*, 309.

[16]   Nunnally, T.; Gutsol, K.; Rabinovich, A.; Fridman, A.; Gutsol, A.; Kemoun, A. *J. Phys. D. Appl. Phys.* **2011**, *44*, 274009.

[17]   Kogelschatz, U. *Plasma Chem. Plasma Process.* **2003**, *23*, 1.

[18]   Kraus, M.; Eliasson, B.; Kogelschatz, U.; Wokaun, A. *Phys. Chem. Chem. Phys.* **2001**, *3*, 294.

[19]   Wang, Q.; Yan, B. H.; Jin, Y.; Cheng, Y. *Energy & Fuels* **2009**, *23*, 4196.

[20]   Tu, X.; Gallon, H. J.; Twigg, M. V.; Gorry, P. A.; Whitehead, J. C. *J. Phys. D. Appl. Phys.* **2011**, *44*, 274007.

[21]   Gallon, H. J.; Tu, X.; Whitehead, J. C. *Plasma Process. Polym.* **2012**, *9*, 90.

[22]   Bill, A.; Wokaun, A.; Eliasson, B.; Killer, E.; Kogelschatz, U. *Energy Convers. Mgmt* **1997**, *38*, S415.

[23]   Eliasson, B.; Kogelschatz, U.; Xue, B.; Zhou, L.-M. *Ind. Eng. Chem. Res.* **1998**, *37*, 3350.

[24]   Kano, M.; Satoh, G.; Iizuka, S. *Plasma Chem. Plasma Process.* **2012**, *32*, 177.

[25]   Futamura, S.; Kabashima, H. in: *Carbon Dioxide Utilization for Global Sustainability, Proceedings of the 7th International Conference on Carbon*

Dioxide Utilization, Elsevier, Amsterdam, **2004**, *153*, 119.

[26] Ihara, T.; Kiboku, M.; Iriyama, Y. *Bull. Chem. Soc. Japan* **1994**, *67*, 312.

[27] Ihara, T.; Ouro, T.; Ochiai, T.; Kiboku, M.; Iriyama, Y. *Bull. Chem. Soc. Japan* **1996**, *69*, 241.

[28] Pinhão, N. R.; Janeco, A.; Branco, J. B. *Plasma Chem. Plasma Process.* **2011**, *31*, 427.

[29] Goujard, V.; Tatibouët, J.-M.; Batiot-Dupeyrat, C. *Plasma Chem. Plasma Process.* **2011**, *31*, 315.

[30] Lindon, M. A.; Scime, E. E. *Front. Phys.* **2014**, *2*, 1.

[31] Ozkan, A.; Dufour, T.; Arnoult, G.; De Keyzer, P.; Bogaerts, A.; Reniers, F. *J. CO_2 Util.* Under review.

[32] Liu, S.; Neiger, M. *J. Phys. D Appl. Phys* **2003**, *36*, 3144.

[33] Pipa, A. V.; Hoder, T.; Koskulics, J.; Schmidt, M.; Brandenburg, R. *Rev. Sci. Instrum.* **2012**, *83*, 075111.

[34] Valdivia-Barrientos, R.; Pacheco-Sotelo, J.; Pacheco-Pacheco, M.; Benítez-Read, J. S.; López-Callejas, R. *Plasma Sources Sci. Technol.* **2006**, *15*, 237.

[35] Lide, D. R. *CRC Handbook of Chemistry and Physics, 85th Ed.*, CRC Press, Boca Raton, **2004**.

[36] Young, K. F.; Frederikse, H. P. R. *J. Phys. Chem. Ref. Data* **1973**, *2*, 313.

[37] Hagelaar, G. J. M.; Pitchford, L. C. *Plasma Sources Sci. Technol.* **2005**, *14*, 722.

[38] Hensel, K.; Katsura, S.; Mizuno, A. *IEEE Trans. Plasma Sci.* **2005**, *33*, 574.

[39] Suib, S. L.; Brock, S. L.; Marquez, M.; Luo, J.; Matsumoto, H.; Hayashi, Y. *J. Phys. Chem. B* **1998**, *102*, 9661.

[40] Albritton, D. L. *Atom. Data Nucl. Data Tables* **1978**, *22*, 1.

[41] Ferguson, E. *Atom. Data Nucl. Data* Tables **1973**, *12*, 159.

[42] Shul, R. J.; Upschulte, B. L.; Passarella, R.; Keesee, R. G.; Castleman, Jr, A. W. *J. Phys. Chem.* **1987**, *91*, 2556.

[43] Van Gaens, W.; Bogaerts, A. *J. Phys. D: Appl. Phys.* **2013**, *46*, 275201.